Journal of Photochemistry and Photobiology A: Chemistry 353 (2018) 34–45

Contents lists available at ScienceDirect

Journal of Photochemistry and Photobiology A: Chemistry

journal homepage: www.elsevier.com/locate/jphotochem

Invited paper

Hydrogen-bonded self-assembly, spectral properties and structure of supramolecular complexes of thiamonomethine cyanines with cucurbit[5,7]urils

Marina V. Fomina[a], Alexander S. Nikiforov[a], Vitaly G. Avakyan[a], Artem I. Vedernikov[a], Nikolai A. Kurchavov[a], Lyudmila G. Kuz'mina[b], Yuri A. Strelenko[c], Judith A.K. Howard[d], Sergey P. Gromov[a,e,*]

[a] Photochemistry Center, Russian Academy of Sciences, Novatorov str. 7A-1, Moscow 119421, Russian Federation
[b] N. S. Kurnakov Institute of General and Inorganic Chemistry, Russian Academy of Sciences, Leninskiy prosp. 31, Moscow 119991, Russian Federation
[c] N. D. Zelinskiy Institute of Organic Chemistry, Russian Academy of Sciences, Leninskiy prosp. 47, Moscow 119991, Russian Federation
[d] Department of Chemistry, Science Laboratories, University of Durham, South Road, Durham DH1 3LE, England, United Kingdom
[e] Department of Chemistry, M. V. Lomonosov Moscow State University, Leninskie Gory 1-3, Moscow 119991, Russian Federation

ARTICLE INFO

Article history:
Received 26 July 2017
Received in revised form 20 October 2017
Accepted 21 October 2017
Available online xxx

Keywords:
Cyanine dyes
Cucurbiturils
Hydrogen-bonded complexes
Stability constants
NMR spectroscopy
Quantum chemical calculations

ABSTRACT

The complex formation of thiamonomethine cyanine dyes bearing two *N*-ammoniohexyl or two *N*-ethyl substituents with cucurbit[5,7]urils (CB[5,7]) in aqueous solutions was studied by electronic and ^{1}H NMR spectroscopy, including spectrophotometric, fluorescence, and ^{1}H NMR titration methods. It was found that CB[5] forms external complexes with the dyes, while CB[7] forms internal (inclusion) complexes of 1:1 and 1(dye):2(CB[5,7]) composition. The complexation with CB[5,7] changes the absorption spectra of cyanine dyes and induces a considerable fluorescence enhancement. The stability constants of the complexes were determined ($\log K_{1:1}$ varies in the range from 3.53 to more than 6, and $\log K_{1:2}$ varies in the range from 3.5 to 4.32). The dye with ammoniohexyl substituents forms more stable complexes owing to hydrogen bond formation between the NH_3^+ groups and the carbonyl groups of the CB[5,7] portals. The structure of supramolecular complexes was confirmed by quantum chemical calculations.

1. Introduction

Cucurbit[*n*]urils (CB[*n*], *n* = 5–10) represent a promising class of macromolecular receptors in supramolecular chemistry. These cavitand molecules are macroheterocycles with a rigid hydrophobic intramolecular cavity and two identical polar portals formed by the carbonyl oxygen atoms. Owing to the specific structural features, CB[*n*] can form stable inclusion complexes of the host–guest type with both neutral molecules and positively charged species such as metal or organic cations [1–8]. The inclusion of an organic dye into the cavitand (host) cavity changes the photochemical properties of the guest molecule: the fluorescence intensity, lifetime, and quantum yield increase, the photostability and disaggregation increase, and so on [9–15]. These photoactive supramolecular systems can be used as fluorescent probes and sensors, for stabilization of laser dyes, for optical information recording systems and so on [16–22].

Previously, we have studied the complex formation of CB[7,8] with 1,2-di(hetaryl)ethylene derivatives [23,24] and cyanine [25,26] and styryl dyes [27–34]. The complex formation has been found to considerably affect the spectral and photochemical properties of the dyes. Indeed, the insertion of a diquinolylethylene derivative into the CB[8] cavity stabilizes its *cis*-isomer [23], while the formation of 2:1 complexes between styryl dyes and CB[8] promotes stereospecific [2 + 2]-photocycloaddition reactions [27,30]. The formation of pseudorotaxane complexes of 4-pyridine-based styryl dyes with CB[7] leads to pronounced enhancement of fluorescence [28–34]. Fluorescence intensity also increases upon the addition of CB[7] to aqueous solutions of trimethine cyanine dyes [25,26].

The presence of ammonioalkyl groups in the dye molecule provides additional options for the dye self-assembly to supramolecular complexes *via* hydrogen bonding with the carbonyl oxygen atoms of the CB[*n*] portals. Indeed, dihetarylethylene derivatives containing two ammonioalkyl groups at nitrogen atoms form

* Corresponding author at: Photochemistry Center, Russian Academy of Sciences, Novatorov str. 7A-1, Moscow 119421, Russian Federation.
E-mail address: spgromov@mail.ru (S.P. Gromov).

https://doi.org/10.1016/j.jphotochem.2017.10.035
1010-6030/

stable inclusion complexes with CB[8] in aqueous solutions (log$K$ > 5), an important role in these complexes being played by hydrogen bonds between the guest ammonium groups and the oxygen atoms of the CB[8] portals [23]. Meanwhile, the complexation between CB[n] and cyanine dyes with terminal ammonium groups in *N*-substituents of heterocyclic residues has not been studied. One can expect a considerable stability increase for these complexes and a noticeable change in the photochemical characteristics of the cyanine dyes.

In this communication, we present the results of electronic and ^{1}H NMR-spectroscopic studies of the self-assembly of complexes formed by CB[5,7] with monomethine cyanine dye **1** containing two *N*-ammoniohexyl groups in the benzothiazole residues and with model compounds, monomethine cyanine dye **2** containing two *N*-ethyl groups and 1,6-hexanediammonium diperchlorate (**3**). The effects of the guest structure and solvent nature on the composition, spatial structure, and stability of the supramolecular complexes with CB[5,7] were elucidated. The structures of the compounds are shown in Fig. 1.

In the series of CB[n], the cavity and portal sizes gradually increase on going from CB[5] to CB[10] at a constant height of 0.91 nm [3]. The structural similarity with different sizes of inner cavities and portals provides selective binding of CB[n] to guest molecules [3,22,35,36]. It is known from the literature that CB[n] form inclusion complexes with alkylammonium and 1,ω-alkanediammonium ions [37–39]. In the series of alkanediammonium ions, which can be considered as structural analogues of the *N*-ammonioalkyl group of type **1** dyes, the dication of compound **3** forms inclusion complexes with CB[6] and larger cucurbiturils [37,38], but the portal width and the cavity volume of CB[5] are insufficient for encapsulation of this cation. In the crystal, CB[5] binds to 1,6-hexanediammonium ions only at the ammonium groups *via* hydrogen bonding with the carbonyl oxygen atoms of the portals of neighboring cavitand molecules, thus forming supramolecular polymers [37,40]. Using X-ray diffraction data for cucurbiturils [3], the 1,6-hexanediammonium dichloride complex with CB[5] [37], and dye **2** (the X-ray diffraction data are described below), it is possible to evaluate in advance their geometric matching for the formation of inclusion complexes (Fig. 1).

Probably, *N*-ammoniohexyl substituents of dye **1** are able to penetrate through CB[7] portals into the cavity, whereas the heterocyclic residue can be only slightly (by the benzene moiety) embedded into CB[7]. Small sizes of CB[5] portals and cavity allow the formation of only “external” complexes with **1**.

2. Experimental

2.1. Materials

3-(6-Ammoniohexyl)-2-{(*Z*)-[3-(6-ammoniohexyl)-1,3-benzothiazol-2(3*H*)-ylidene]methyl}-1,3-benzothiazol-3-ium triperchlorate (**1**), 1,6-hexanediammonium diperchlorate (**3**), 3-ethyl-2-methyl-1,3-benzothiazol-3-ium iodide (**4**), and 3-ethyl-2-(ethylsulfanyl)-1,3-benzothiazol-3-ium 4-methylbenzenesulfonate (**5**)

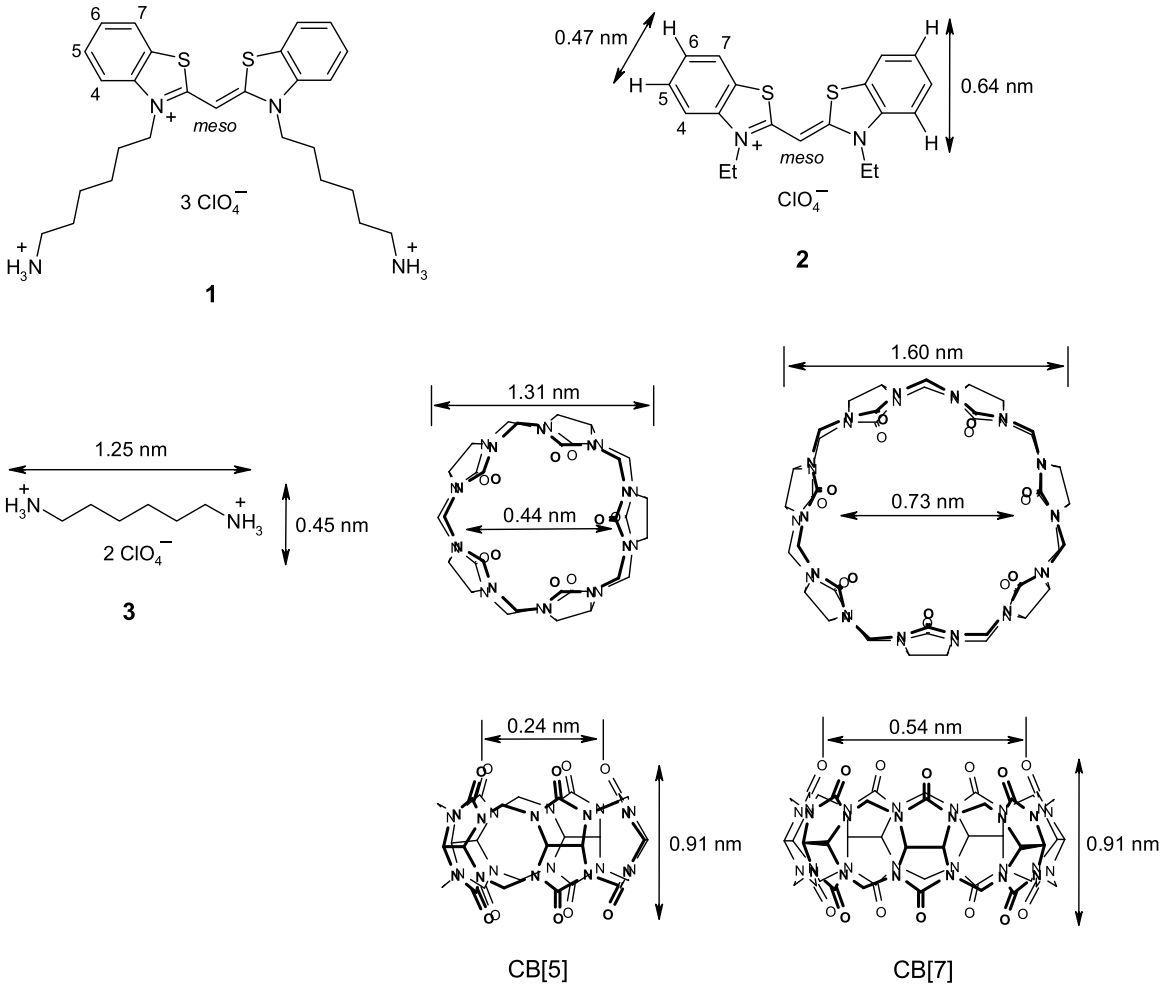

Fig. 1. Structures of the studied guest molecules **1**–**3** and host molecules CB[5] and CB[7].

were prepared by known procedures [41–44]. CB[7]·13H_2O and CB [5]·2.5KCl·3.4H_2O were used as received (Aldrich). Distilled water (HPLC grade, Aldrich) and MeCN (extra high purity, Cryochrom) were used to prepare solutions.

*2.1.1. 3-Ethyl-2-[(Z)-(3-ethyl-1,3-benzothiazol-2(3H)-ylidene) methyl]-1,3-benzothiazol-3-ium perchlorate (**2**)*

A mixture of salts **4** (153 mg, 0.5 mmol) and **5** (198 mg, 0.5 mmol) was dissolved in abs. EtOH (3 mL) at heating and then triethylamine (140 μL, 1 mmol) was added to this solution. The reaction mixture was stirred under reflux for 1 h and then cooled to room temperature. The precipitate that formed was collected on a filter, washed with a mixture of EtOH (10 mL) and water (10 mL) and with diethyl ether, and dried in air to give the iodide salt of the dye. The iodide salt (153 mg, 0.3 mmol) was dissolved in EtOH (100 mL) at heating and $HClO_4$ (70% (aq.), 30 μL, 0.36 mmol) was added to the solution. After cooling to −10 °C, the yellow precipitate that formed was collected on a filter, washed with cold EtOH and diethyl ether, and dried in air to give **2** (138 mg, yield 63%), mp 310–312 °C. UV–vis (MeCN) λ_{max} 423 nm (ε 81100 L mol^{-1} cm^{-1}); fluorescence (MeCN, λ_{ex} 415 nm) λ^{fl}_{max} 473 nm ^{1}H NMR (500 MHz, DMSO-d_6, 30 °C) δ: 1.37 (t, 6H, J = 7.1 Hz, 2 *Me*CH_2), 4.66 (q, 4H, J = 7.1 Hz, 2 *C*H_2Me), 6.70 (s, 1H, *meso*-H), 7.47 (m, 2H, 2 6-H), 7.65 (m, 2H, 2 5-H), 7.86 (d, 2H, J = 8.0 Hz, 2 4-H), 8.18 (d, 2H, J = 8.0 Hz, 2 7-H). ^{13}C NMR (125 MHz, DMSO-d_6, 25 °C) δ: 12.12 (2 *Me*CH_2), 41.43 (2 *C*H_2Me), 81.75 (*meso*-C), 113.45 (2 4-C), 123.41 (2 7-C), 124.80 (2 6-C), 124.88 (2 7a-C), 128.50 (2 5-C), 139.61 (2 3a-C), 161.26 (2-C). Anal. calcd. for $C_{19}H_{19}ClN_2O_4S_2$: C, 51.99; H, 4.36; N, 6.38; found: C, 51.93; H, 4.47; N, 6.20.

2.2. Methods

Melting points were measured on a Mel-Temp II instrument. Elemental analysis was carried out at the Microanalytical Laboratory of the A. N. Nesmeyanov Institute of Organoelement Compounds (Russian Academy of Sciences, Moscow). The sample for elemental analysis was dried at 80 °C *in vacuo*.

2.2.1. X-ray diffraction experiment

The single crystal of dye 2 was obtained by slow evaporation of a solution of the dye in a CHCl3–CH2Cl2–MeCN mixture at ambient temperature. The crystal was coated with perfluorinated oil and mounted on a Bruker SMART-CCD diffractometer (graphite monochromatized Mo-Kα radiation (= 0.71073 Å), (scan mode) under a stream of cooled nitrogen. The set of experimental reflections was measured and the structure was solved by direct methods and refined by the full matrix least-squares against F2 with anisotropic thermal parameters for all non-hydrogen atoms (except for most oxygen atoms of disordered perchlorate anion). The hydrogen atoms were fixed at calculated positions at carbon atoms and then refined using a riding model. The perchlorate anion is disordered over two positions with occupancy ratio of 0.55:0.45. All the calculations were performed using the SHELXL-2014 software [45]. The crystal parameters and structure refinement details are given in Table 1. Crystallographic data for the structure have been deposited with the Cambridge Crystallographic Data Centre as supplementary publication no. CCDC-1560259. A copy of the data can be obtained, free of charge, on application to CCDC, 12 Union Road, Cambridge CB2 1EZ, UK, (fax: +44(0)1223 336033 or e mail: deposit@ccdc.cam.ac.uk).

2.2.2. NMR spectroscopy measurements and titration

^{1}H and ^{13}C NMR spectra were recorded on a Bruker DRX500 spectrometer in DMSO-d_6 and a D_2O–MeCN-d_3 mixture (10:1, v/v) at 25–30 °C with the DMSO-d_5 or HOD signal as the internal standard (δ_H 2.50 or 4.70, respectively; δ_C 39.43 for DMSO-d_6). In

Table 1
Crystallographic data and structure refinement details for **2.**

Parameter	**2**
Empirical formula	$C_{19}H_{19}ClN_2O_4S_2$
Formula weight	438.93
Crystal system	Monoclinic
Space group	$P2_1/n$
Temperature (K)	120(2)
Unit cell: dimensions (Å), (°)	a = 7.3755(8), b = 25.420(3), c = 10.3164(11) α = 90, β = 92.492(7), γ = 90
Volume (Å^3)	1932.3(4)
Z, D_{calcd} (Mg m^{-3})	4, 1.509
μ (mm^{-1})	0.443
F(000)	912
Crystal size (mm^3)	0.80 × 0.02 × 0.02
θ Range (°)	1.60–27.99
Index ranges	$-9 \le h \le 9$, $-33 \le k \le 33$, $-13 \le l \le 13$
Reflections collected	18592
Independent reflections	4661 (R_{int} = 0.3103)
Reflections with $I > 2\sigma(I)$	1631
Completeness to theta = 25.24°	99.8%
Goodness-of-fit on F^2	0.777
Final R indices [$I > 2\sigma(I)$]	R_1 = 0.0734, wR_2 = 0.1036
R indices (all data)	R_1 = 0.2341, wR_2 = 0.1321
Largest diff. peak and hole (e·Å^{-3})	0.512 and −0.523
Data/restraints/parameters	4661/0/253

^{1}H NMR titration, the compositions and stability constants of the complexes of dyes **1**, **2** and 1,6-hexanediammonium diperchlorate (**3**) with CB[5,7] were determined by analyzing the changes in the positions of the H signals ($\Delta\delta_H$) of the dye (or compound **3**) depending on the concentration ratio of CB[5,7] and the dye (or compound **3**). The CB[5,7] concentration was varied in the range from 0 to 1×10^{-3} mol L^{-1}, while the overall concentration of dye (or compound **3**) did not change, being equal to $\sim 5 \times 10^{-4}$ mol L^{-1}. The $\Delta\delta_H$ values were measured to an accuracy of 0.001 ppm with correction for MeCN-d_2 signal shift. The stability constants of the complexes were calculated using the HYPNMR program [46].

2.2.3. Optical spectroscopy measurements and titrations

The absorption spectra of dyes **1**, **2** were recorded on a Cary 4000 (Agilent) spectrophotometer. Fluorescence spectra of dyes **1**, **2** were measured on a Shimadzu RF-5301PC spectrofluorimeter. All the spectra were recorded in MeCN at room temperature. The spectrophotometric and fluorescence titrations were performed in a water–MeCN mixture (10:1, v/v) and in water at room temperature. The compositions and stability constants of the complexes of dyes **1**, **2** with CB[5,7] were determined by analyzing the changes in the absorption and fluorescence spectra of the dye depending on the concentration ratio of CB[5,7] and the dye. In spectrophotometric titration, the CB[5,7] concentration was varied in the range from 0 to 4×10^{-4} mol L^{-1}, while the overall concentration of dye remained equal to $\sim 5 \times 10^{-6}$ mol L^{-1} in water. In the fluorescence titration, the CB[5,7] concentration was varied in the range from 0 to 1.5×10^{-4} mol L^{-1}, the overall concentration of dye **1** was 5×10^{-6} mol L^{-1}, and the concentration of dye **2** remained equal to $\sim 5 \times 10^{-6}$ mol L^{-1}. The stoichiometry and stability constants of complexes were calculated using HypSpec software (Hyperquad program package) [47].

2.2.4. Quantum chemical modeling

Quantum chemical calculations for dye **1** and complexes of **1** with CB[5] and CB[7] were carried out by the PM6-DH+ semiempirical method implemented in the MOPAC 2012 program package [48,49]. In this method, parameterization includes the dispersion (van der Waals) corrections and improves the prediction of hydrogen bond energies. This parametrization is necessary, because after complex formation, the dye is retained in the cavity

by electrostatic and van der Waals forces. The complex formation energy, $E_{compl\text{-}form}$, was calculated as the difference between the heat of formation of the complex, ΔH_f, the structure of which was first fully optimized, and the sum of ΔH_f values for the dye and the cavitand.

The calculation for isolated complexes formed by dye **1** with CB[5] and CB[7] provided answers to the following questions: (1) whether **1** can penetrate into the CB[5] cavity and be retained there; if not, what is the most probable structure of complex **1**·CB[5]; (2) what is the most probable structure of the inclusion complex **1**@CB[7]. An important reason in favor of calculations for isolated inclusion complexes is related to numerous resemblances of calculated structures with those determined by X-Ray diffraction analysis and contained in the CCSD. This means that structures of this type actually do exist and are energetically more favorable than other types of complexes that might occur in aqueous solutions. Furthermore, the existence of inclusion complexes **1** is confirmed by experimental spectral data obtained in the present study (see below).

3. Results and discussion

3.1. Synthesis of dye 2

To investigate the possibility of constructing photoactive supramolecular systems based on CB[*n*] and monomethine cyanine dyes and the effect of their structures on the properties of supramolecular complexes, we synthesized a model benzothiazole dye **2** containing ethyl substituents at the nitrogen atoms. Dye **2** was prepared using a reported procedure [50] by condensation of heterocyclic salts **4** and **5** in ethanol under the action of triethylamine (Scheme 1). The yield of **2** was 63%.

3.2. X-ray diffraction study of 2

Dye **2** was prepared as a single crystal, which was studied by X-ray diffraction. This structure is shown in Fig. 2. The chromophore moiety of the organic cation is planar: the dihedral angle between the planes of the heterocyclic residues in molecule **2** is only 2.5°. The bond lengths in the C(7)–C(8)–C(9) monomethine chain are nearly equal [1.388(6) and 1.385(7) Å], which attests to

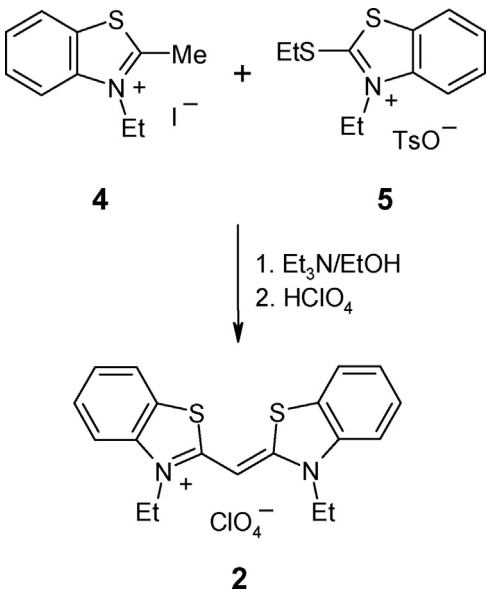

Scheme 1. Synthesis of dye **2**.

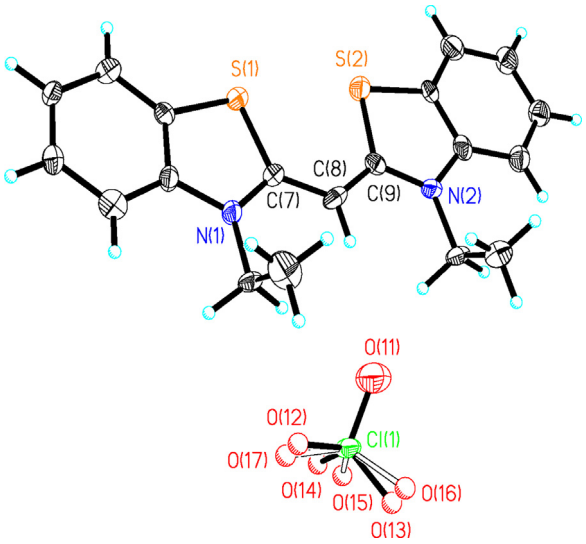

Fig. 2. Structure of **2**. All non-hydrogen atoms are shown at the 50% probability level of their anisotropic thermal parameters (except for most O atoms of the disordered anion).

efficient conjugation. Both CH_2N groups and the *meso*-hydrogen atom point to the same direction and are located within the plane of the conjugated moiety. This is a typical cyanine dye geometry in the crystals [41,51–54]. It follows from NMR spectroscopy data that this geometry is also retained in solution, as indicated by intense cross-peaks between the *meso*-hydrogen atoms and the CH_2N-group protons in the NOESY spectra of the dyes [41].

The dye cations in the crystal are arranged in tilted stacks with a centrosymmetric organization; the stacking interactions in these stacks involve mainly the benzothiazolium residues. The distance between the planes of the conjugated moieties of cations **2** adjacent in the stack is ~3.3 Å.

3.3. ^{1}H NMR spectroscopy

The complexation of dye **1** and model compound **3** with CB[5,7] was studied by ^{1}H NMR spectroscopy. For the use of this method, working concentrations of compounds should be not less than 5×10^{-4} mol L^{-1}. The required solubility of components was attained by using a mixture of D_2O and MeCN-d_3 in 10:1 ratio (v/v) as the solvent. For systems containing dye **2**, we were unable to select a solvent mixture that would dissolve the required amounts of both components.

The formation of supramolecular complexes induces noticeable changes in the ^{1}H NMR spectra of guest molecules [14,15,20,23,24,29,32,39]. Gradual increase in the concentration of CB[5] in a solution containing compound **3** results in monotonic downfield shifts of the methylene proton signals of guest molecules ($\Delta\delta_H$ up to 0.02 ppm) (Fig. 3*a*). Apparently, the guest protons are located outside the CB[5] cavity but within the deshielding area of the carbonyl groups that form the cavitand portals, although occur at some distance from the latter. Conversely, mixing of **3** with CB[7] induces considerable upfield shifts of the signals of guest methylene protons ($\Delta\delta_H$ up to −0.81 ppm) (Fig. 3*b*). This implies that these protons are located inside the CB[7] cavity and are shielded by the electron-donating cavity walls.

Thus, it follows from NMR data that compound **3**, which is a structural analogue of the *N*-ammoniohexyl substituents of dye **1**, forms a host–guest inclusion complex with CB[7], whereas in the case of CB[5], dication **3** is located outside the cavity of the cavitand.

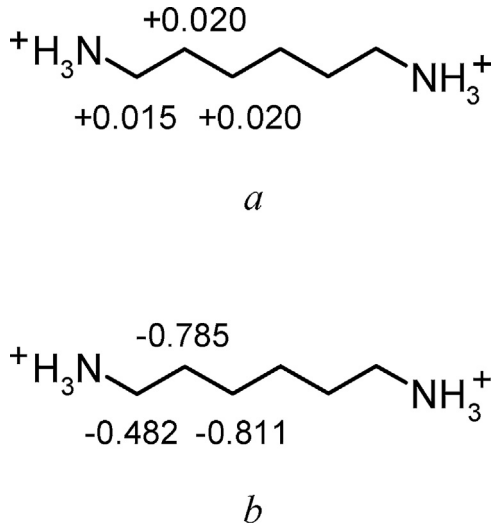

Fig. 3. Changes in the proton chemical shifts, $\Delta\delta_H = \delta_H$(**3**/CB[*n*] mixture) − δ_H(free **3**), of compound **3** upon the addition of CB[5] (*a*) and CB[7] (*b*) (1(**3**):2(CB[*n*]) ratio), D_2O–MeCN-d_3 (10:1, v/v), 25 °C.

Upon the addition of excess CB[5] to dye **1**, the ^{1}H NMR spectrum shows slight downfield shifts of signals of ammoniohexyl protons and the *meso*-proton of **1** (Figs. 4 , 5*a*); the proton signals of the heterocyclic residues have low sensitivity to the presence of CB[5]. This means that all aliphatic protons and the *meso*-proton of the dye are located outside the CB[5] cavity and fall into the deshielding region of the portal carbonyl groups, similarly to the situation in the system **3**/CB[5]. The results provide the conclusion that **1**·CB[5] is an external complex.

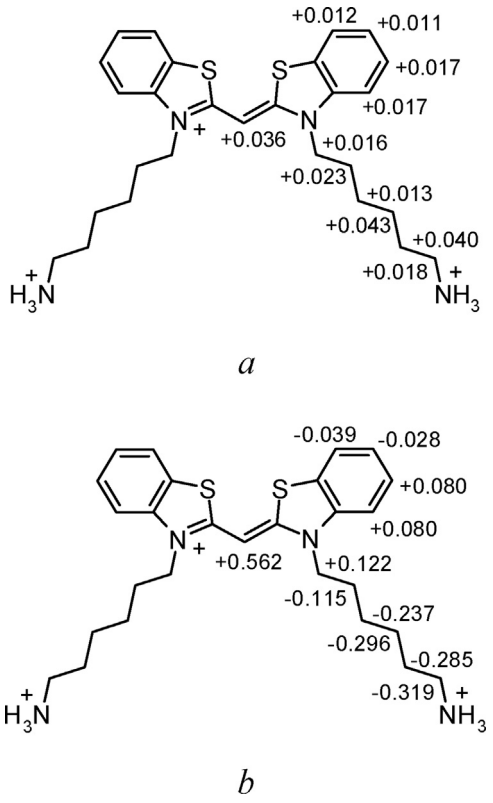

Fig. 5. Changes in the proton chemical shifts, $\Delta\delta_H = \delta_H$(**1**/CB[*n*] mixture) − δ_H(free **1**), of dye **1** ($C_{\mathbf{1}} = 5 \times 10^{-4}$ mol L^{-1}) upon the addition of CB[5] (*a*) and CB[7] (*b*) ($C_{CB[n]} = 1 \times 10^{-3}$ mol L^{-1}), D_2O–MeCN-d_3 (10:1, v/v).

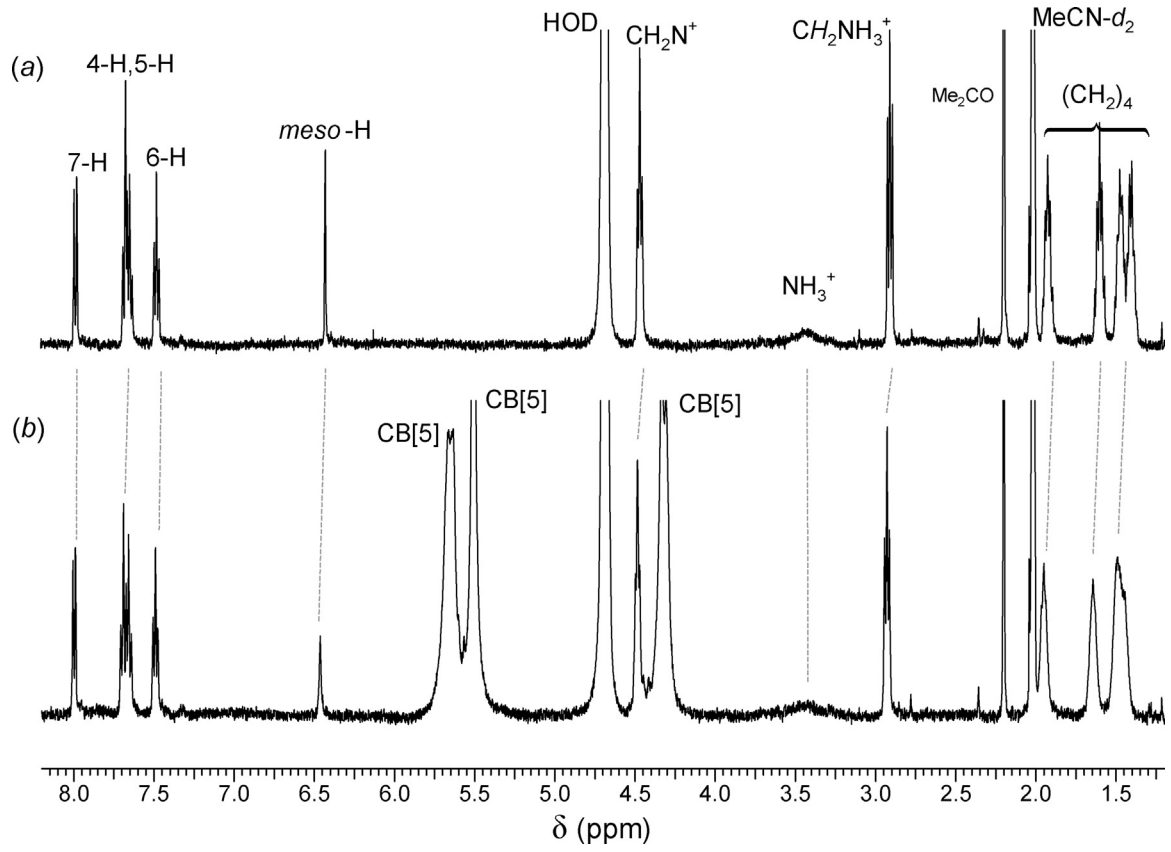

Fig. 4. ^{1}H NMR spectra of (*a*) **1** and (*b*) a mixture of **1** and CB[5] ($C_{\mathbf{1}} = 5 \times 10^{-4}$ mol L^{-1}, $C_{CB[5]} = 1 \times 10^{-3}$ mol L^{-1}), D_2O–MeCN-d_3 (10:1, v/v), 30 °C.

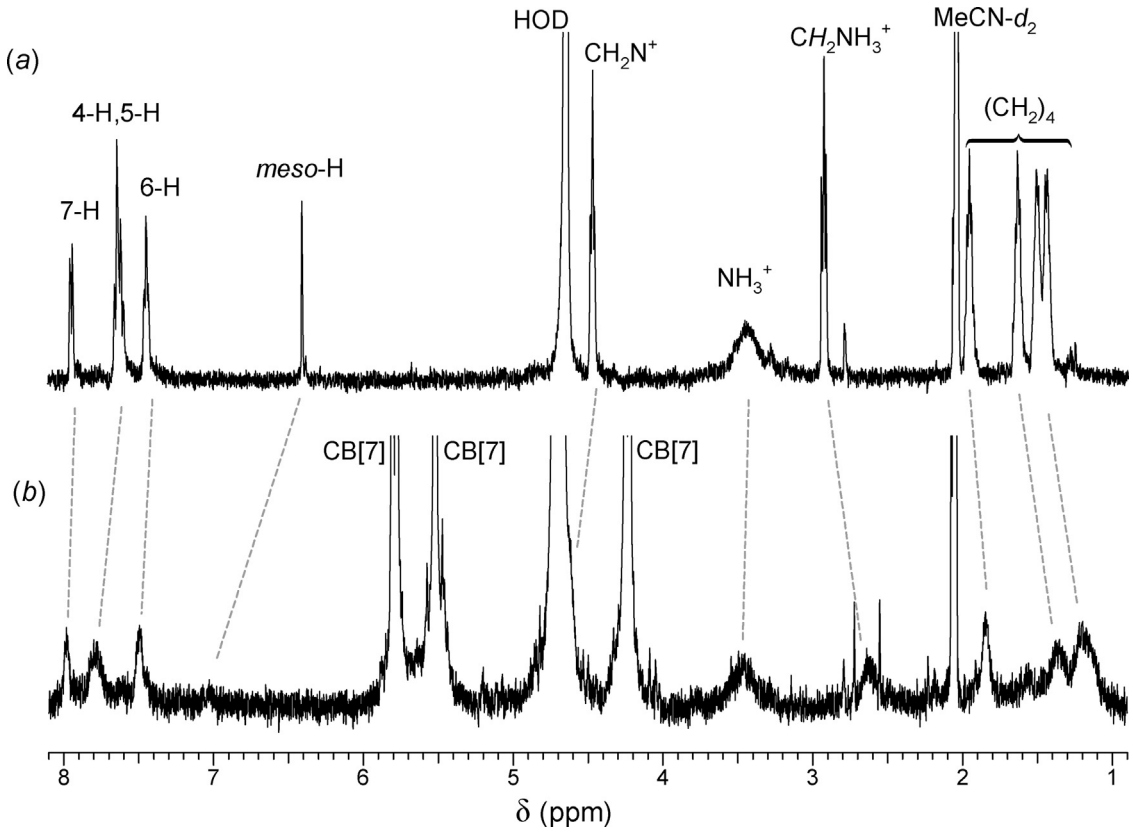

Fig. 6. ^{1}H NMR spectra of (*a*) **1** and (*b*) a mixture of **1** and CB[7] ($C_{\mathbf{1}} = 5 \times 10^{-4}$ mol L^{-1}, $C_{CB[7]} = 1 \times 10^{-3}$ mol L^{-1}), D_2O–MeCN-d_3 (10:1, v/v), 27 °C.

The complex formation occurs apparently *via* hydrogen bonding between the ammoniohexyl NH_3^+ groups of dye **1** and the carbonyl oxygen atoms of the CB[5] portals.

When excess CB[7] is added to a solution of **1**, the ^{1}H NMR spectral pattern differs from that for CB[5]. Most of the proton signals of the ammoniohexyl groups shift upfield ($\Delta\delta_H$ up to -0.32 ppm), whereas signals of the 4-H and 5-H heterocyclic residues shift downfield ($\Delta\delta_H$ up to 0.08 ppm). The *meso*-proton signal experiences a large downfield shift ($\Delta\delta_H = 0.56$ ppm) (Figs. 5*b*, 6). Considering the determined $\Delta\delta_H$ values for various protons of the guest, one can suggest the most probable structure of complex **1**@CB[7]: one ammoniohexyl substituent of the dye is embedded into the cavity, whereas the rest of the organic trication is situated outside. The CH_2N groups and *meso*-H atoms are located most closely to the CB[7] portals, which results in noticeable downfield shifts of their signals.

According to Fig. 1, the length of the ammoniohexyl group is sufficient for this group to penetrate all the way through the CB[7] cavity, so that the ammonium ion is located in the vicinity of the opposite portal and can be hydrogen-bonded to the carbonyl oxygen atoms of this portal, which should make an additional contribution to the stability of **1**@CB[7].

The stability of the complexes was determined by means of ^{1}H NMR titration (see application of this method to CB[*n*]-based supramolecular systems in [23,24,29,32]). At any **1**,**3**/CB[5,7] ratios, the spectra exhibited averaged (in some cases, broadened) proton signals for the complex and the free components, which may be attributable to exchange processes that are relatively fast on the ^{1}H NMR time scale. The stability constants of the complex were determined by analyzing the dependence of the shifts of proton signals ($\Delta\delta_H$) of the guest molecules on the concentration of the cavitand added.

In all cases, the $\Delta\delta_H - C_{CB[5,7]}/C_{\mathbf{1,3}}$ dependences were adequately described by the reaction model comprising one equilibrium (*1*).

$$\mathbf{1},\mathbf{3} + CB[5,7] \overset{K_{1:1}}{\rightleftarrows} \mathbf{1},\mathbf{3}\cdot CB[5,7] \quad (1)$$

where $K_{1:1}$, M^{-1} is the stability constant of the 1:1 complex.

The stability constants of complexes of **1** and **3** with CB[5] and CB[7] were found by processing the ^{1}H NMR titration data considering equilibrium (*1*); the $\log K_{1:1}$ values are presented in Table 2.

Analysis of the data of Table 2 demonstrated that the most stable and, most likely, inclusion complexes are formed with CB[7]. Note that increasing positive charge in the trication of dye **1** leads to higher stability of the complex of **1** with CB[7] as compared with the analogous complex of dication **3**.

3.4. Optical spectroscopy measurements

The complexation of dyes **1** and **2** with CB[5,7] was studied by electronic spectroscopy using a water–MeCN mixture (10:1, v/v) and water as solvents.

Table 2
Stability constants of complexes of **1** and **3** with CB[5,7].[a]

Compound	$\log K_{1:1}$ [b]	
	CB[5]	CB[7]
1	3.5	4.3
3	–[c]	3.7

[a] ^{1}H NMR titration, D_2O–MeCN-d_3 (10:1, v/v), 25 °C.
[b] The experimental error of measurement of $K_{1:1}$ is ±30%.
[c] The stability constant of the complex could not be determined because of too small spectral changes.

Table 3
Stability constants of the complexes of dyes **1** and **2** with CB[5,7].[a]

Solvent	Complex	Spectrophotometric titration		Fluorescent titration	
		$\log K_{1:1}$	$\log K_{1:2}$	$\log K_{1:1}$	$\log K_{1:2}$
water–MeCN (10:1, v/v)	**1**·CB[5]	3.53		3.93	
	1@CB[7]	4.03		4.44	
water	**2**·CB[5]	3.70		3.82	
	2@CB[7]	>3.6 [b]		>3.4 [b]	
	1·CB[5]	5.58	4.32	5.2 [c]	3.5 [c]
	1@CB[7]	>6	3.96	>6	3.75

[a] Room temperature; experimental error of measurement of $K_{1:1}$ and $K_{1:2}$ is ±20%.
[b] The underestimated $\log K_{1:1}$ values are related to the presence of the complex $(\mathbf{2})_2$@$(CB[7])_2$ in the equilibrium.
[c] Low-precision log*K* values due to minor spectral changes.

For correction and comparison of the complexation constants found by ^{1}H NMR titration, we first carried out the spectrophotometric and fluorescence titration of **1**,**2**/CB[5,7] systems in a water–MeCN mixture (*cf.* use of this method in [29,32]). In the **1**/CB[5,7] systems, the spectral changes during the titration were slight, but clear-cut, whereas in the **2**/CB[5,7] systems, the changes were negligibly small, which precluded determination of the stability of possible complexes **2**·CB[5,7].

The dependence of changes in the absorption and fluorescence spectra of dye **1** on the concentration of CB[5,7] is well described by a model taking account of equilibrium of type (*1*). The stability constants of the complexes of dye **1** with CB[5,7] are presented in Table 3.

It follows from the data of Tables 2 and 3 that the stability constants of complexes **1**·CB[5] and **1**@CB[7] determined by spectrophotometric, fluorescence, and ^{1}H NMR titration procedures are in good agreement to within the experimental error. This allows for correct comparison of the $K_{1:1}$ values found by different methods for all the compounds in question, even in the case where one of the methods does not give a definite result for objective reasons (for example, because of too minor spectral changes or for a compound devoid of a chromophore moiety, such as compound **3**). Relatively small changes that occur in the absorption and fluorescence spectra upon the formation of complexes **1**·CB[5] and **1**@CB[7] in a water–MeCN mixture are caused by the fact that the presence of MeCN in a solvent mixture markedly decreases the stability of complexes **1**,**2**·CB[5] and **1**,**2**@CB[7]. Previously, we observed a similar effect of MeCN on the stability of inclusion complexes of 4-styrylpyridines with CB[7] [32]. Apparently, MeCN molecules compete with the guest molecules for the hydrophobic cucurbituril cavities [4].

In order to eliminate the effect of MeCN on the stability of the complexes, we studied the complexation of dyes **1** and **2** with CB[5,7] in water.

Gradual addition of CB[5] to an aqueous solution of dye **2** induces a regular decrease in the intensity of the long-wavelength absorption band, which implies the formation of complex **2**·CB[5] (Fig. 7*a*).

The absorption spectrum of dye **2** in MeCN exhibits one intense long-wavelength band with λ_{max} = 423 nm. In the spectrum of **2** in water, apart from the long-wavelength band with λ_{max} = 422 nm corresponding to monomer **2**, a new blue-shifted low-intensity band appears as a shoulder at ~407 nm (Fig. 7*a*, inset). Cyanine dyes in aqueous solutions are known to be prone to dimerization and aggregation [55,56]. The formation of dye dimers is accompanied by the appearance of a second spectral band, which tends to undergo a blue shift relative to the band of monomers [57,58]. The inset of Fig. 7*a* shows the increase in the absorption at 407 nm with increasing the concentration of **2** (i.e., 10-fold, the absorption spectra are normalized to the absorbance at the monomer absorption maximum at 422 nm). In other words, the increase in the dye concentration shifts the monomer (M)–dimer (D) equilibrium towards the dimer.

Upon the addition of excess CB[7] to an aqueous solution of dye **2**, we detected a considerable decrease in the intensity of the long-wavelength absorption band at λ_{max} = 422 nm accompanied by a 3 nm red shift and appearance of a new band as a shoulder at ~407 nm (Fig. 7*b*). These spectral changes are apparently due to both the formation of an inclusion complex with the dye monomer, **2**@CB[7], and the formation of the dimeric complex $(\mathbf{2})_2$@$(CB[7])_2$. It is known that cyanine dyes and CB[7] can form 2:2 dimeric complexes [26]. We were unable to calculate simultaneously the

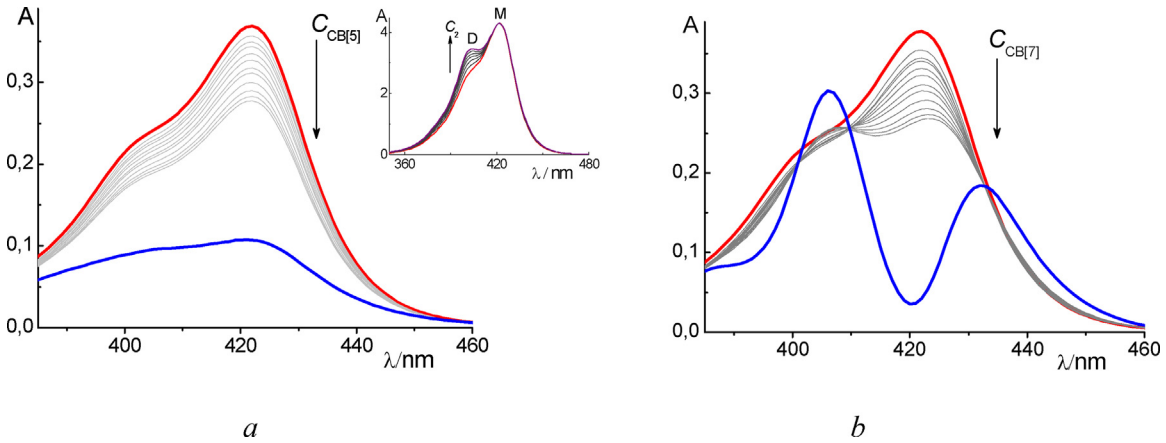

a *b*

Fig. 7. Changes in the absorption spectra of dye **2** ($C_2 = 4.6 \times 10^{-6}$ mol L^{-1}) in water depending on the concentrations of CB[5] (*a*) or CB[7] (*b*) added ($C_{CB[5,7]}$ varies from 0 to 1×10^{-4} mol L^{-1}). The blue curves are the simulated spectra of complexes **2**·CB[5] and **2**@CB[7]; the red curves are the spectra of the free dye. Inset: concentration dependence of the absorption spectra of **2** in water. C_2 varies from 5×10^{-6} mol L^{-1} to 5×10^{-5} mol L^{-1}); the spectra are normalized at the absorption maximum of the monomer. (For interpretation of the references to colour in this figure legend, the reader is referred to the web version of this article.)

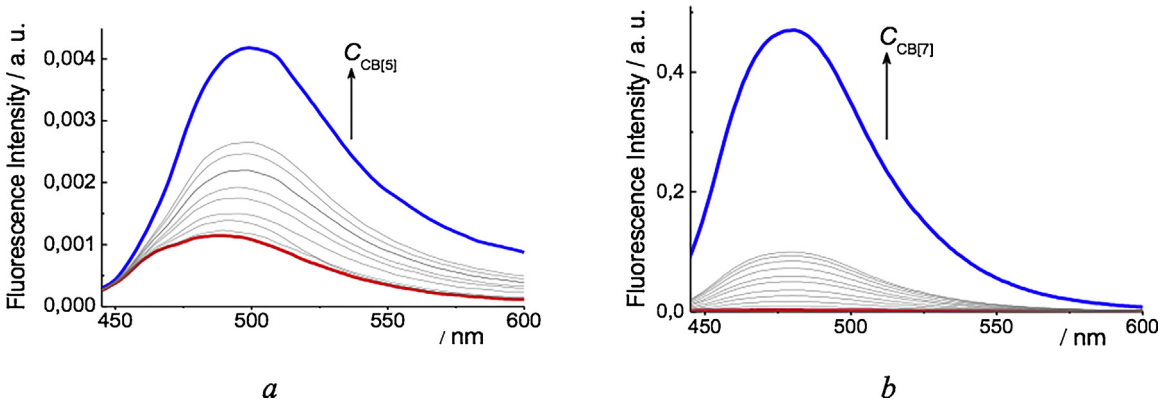

Fig. 8. Changes in the fluorescence spectra of dye **2** ($C_{\mathbf{2}} = 4.6 \times 10^{-6}$ mol L^{-1}) in water depending on the concentrations of CB[5] (*a*) and CB[7] (*b*) added ($C_{CB[5,7]}$ varies from 0 to 1×10^{-4} mol L^{-1}). The fluorescence was excited by light at 390 nm (*a*) and 410 nm (*b*). The blue curves are the simulated spectra of complexes **2**·CB[5] and **2**@CB[7]; the red curves are the spectra of the free dye. (For interpretation of the references to colour in this figure legend, the reader is referred to the web version of this article.)

Table 4
Spectral properties of dyes **1** and **2** and their mixtures with excesses of CB[5,7].

Solvent	Substance	λ^{abs}_{max} (nm)	λ^{fl}_{max} (nm)	$I^{fl}_{\mathbf{1,2}/CB[5,7]}/I^{fl}_{\mathbf{1,2}}$
water–MeCN	**1**	424	471	
	1/CB[5][a]	425	481	1.8
	1/CB[7][a]	425	473	7.4
water	**1**	424	475	
	1/CB[5][b]	424	484	1.9
	1/CB[7][b]	427	477	11.3
	2	422	471	
	2/CB[5][b]	421	478	1.3
	2/CB[7][b]	425	478	55

[a] $C_{CB[5,7]}/C_{\mathbf{1,2}}$ is 5 for absorption spectra and 20 for fluorescence spectra.
[b] $C_{CB[5,7]}/C_{\mathbf{1,2}}$ is 20 for the absorption and fluorescence spectra.

stability constants of the probable complexes **2**@CB[7] and $(\mathbf{2})_2$@$(CB[7])_2$. We assume that the log$K_{1:1}$ value that we found for complex **2**@CB[7] is underestimated due to the presence of complex $(\mathbf{2})_2$@$(CB[7])_2$ in the equilibrium (Table 3). Furthermore, during the titration, the ratio of the monomer and dimer of dye **2** is evidently changed in favor of the dimer as the CB[7] concentration increases; this introduces an additional error in the calculation of the stability constant $K_{1:1}$.

In **2**/CB[5] and **2**/CB[7] mixtures in water, the fluorescence intensity increased up to 1.3- and 55-fold, respectively, in comparison with the free dye (Fig. 8, Table 4).

Also, as in the case of model dye **2**, the formation of complexes between dye **1** and CB[5] in water induces noticeable changes in the absorption and fluorescence spectra (Figs. 9 *a*, 10*a*). Despite the fact that the dye chromophore is evidently located outside the cavity, the spatial proximity of CB[5] and the chromophore has a rather pronounced effect on the latter. Complex **1**·CB[5] is almost two orders of magnitude more stable than complex **2**·CB[5] (see Table 3). Apparently, hydrogen bonding between the ammonium groups of the *N*-substituents of dye **1** and the carbonyl oxygen atoms of the CB[5] portal makes a considerable additional contribution to the stability of complex **1**·CB[5].

The gradual increase in the content of CB[7] in the aqueous solution during spectrophotometric titration of dye **1** induces first a red shift of the long-wavelength absorption band maximum by 1 nm and decrease in the absorbance, while further increase in the CB[7] concentration in a solution of **1** leads to an additional red shift of the long-wavelength absorption band maximum by 3 nm, but the band intensity becomes higher (Fig. 9*b*). This spectral behavior can be attributed to the formation of two types of inclusion complexes of 1:1 and 1:2 compositions.

The considerable differences between the simulated absorption spectra of complexes **1**@CB[7] and **2**@CB[7] can be attributed to the fact that complex **1**@CB[7] does not form dimers. Indeed, as can be seen in the inset of Fig. 9*a*, the trication of dye **1**, unlike the monocation of dye **2**, does not tend to be aggregated, obviously, because of the Coulomb repulsion.

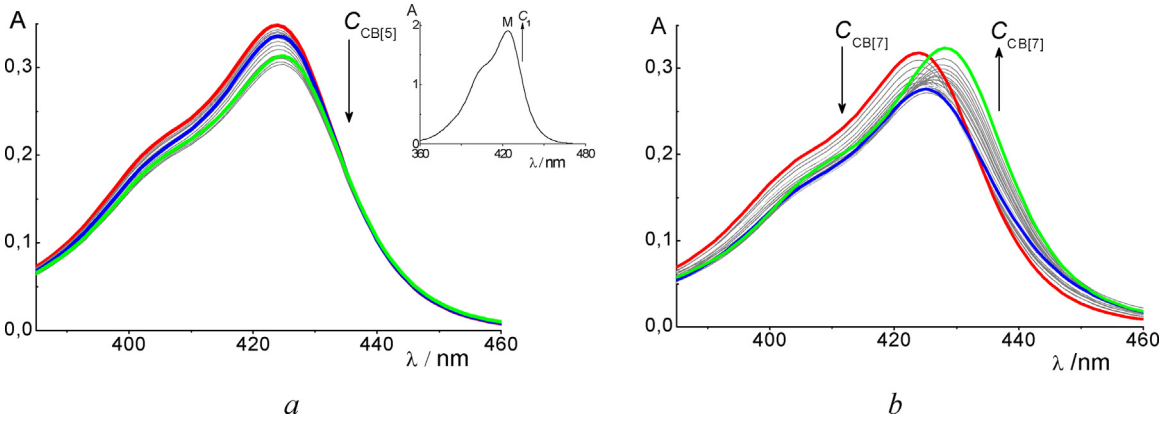

Fig. 9. Changes in the absorption spectra of dye **1** ($C_{\mathbf{1}} = 5 \times 10^{-6}$ mol L^{-1}) in water depending on the concentrations of CB[5] ($C_{CB[5]}$ varies from 0 to 1.8×10^{-4} mol L^{-1}) (*a*) and CB[7] added ($C_{CB[7]}$ varies from 0 to 3.8×10^{-4} mol L^{-1}) (*b*). The blue curves are the simulated spectra of complexes **1**·CB[5] and **1**@CB[7], the green curves are the simulated spectra of complexes **1**·$(CB[5])_2$ and **1**@$(CB[7])_2$, and the red curves are the spectra of the free dye. Inset: concentration dependence of the absorption spectra of **1** in water ($C_{\mathbf{1}}$ varies from 5×10^{-6} mol L^{-1} to 5×10^{-5} mol L^{-1}); the spectra are normalized at the absorption maximum. (For interpretation of the references to colour in this figure legend, the reader is referred to the web version of this article.)

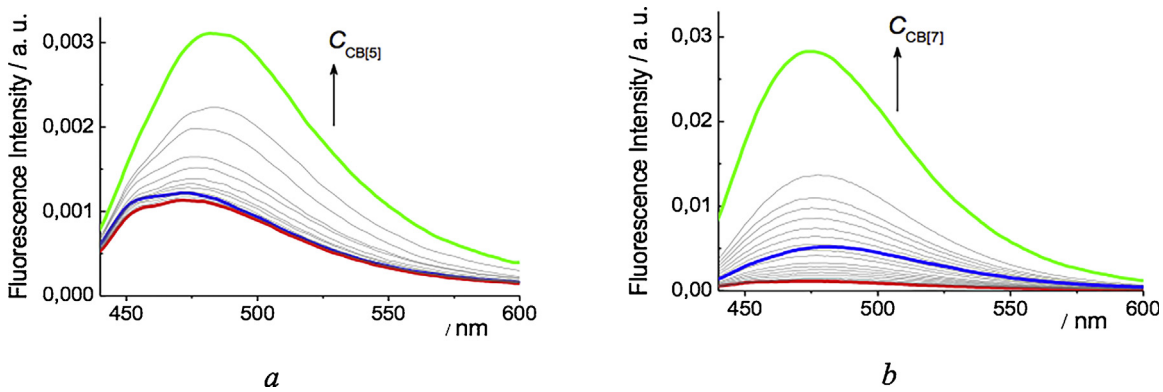

Fig. 10. Changes in the fluorescence spectra of dye **1** ($C_1 = 5 \times 10^{-6}$ mol L^{-1}) in water depending on the concentrations of CB[5] ($C_{CB[5]}$ varies from 0 to 1.5×10^{-4} mol L^{-1}) (*a*) and CB[7] added ($C_{CB[7]}$ varies from 0 to 1.5×10^{-4} mol L^{-1}) (*b*). The fluorescence was excited by light at 390 nm. The blue curves are the simulated spectra of complexes **1**·CB[5] and **1**@CB[7], the green curves are the simulated spectra of complexes **1**·(CB[5])$_2$ and **1**@(CB[7])$_2$, and the red curves are the spectra of the free dye. (For interpretation of the references to colour in this figure legend, the reader is referred to the web version of this article.)

Like in the case of complex **1**·CB[5], the hydrogen bonding between the *N*-substituent ammonium groups of dye **1** and the carbonyl oxygen atoms of the CB[7] portal makes a considerable contribution to the stability of complex **1**@CB[7] (Table 3).

For the **1**/CB[7] mixture in water, the fluorescence intensity markedly increases with respect to that of free dye (Fig. 10*b*, Table 4). The fluorescence enhancement may be a consequence of a more "rigid" environment of the dye chromophore when complexed with CB[7], which hampers the internal conversion of the excited molecule to the ground state.

For comparison, Table 4 presents the spectral properties of dyes **1** and **2** and their changes for mixtures with CB[5,7].

Using the results of spectrophotometric and fluorescence titration in water in terms of equilibria (*2*) and (*3*), the stability constants of the complexes were determined. The results are presented in Table 3.

$$\mathbf{1},\mathbf{2} + \mathrm{CB}[5,7] \overset{K_{1:1}}{\rightleftarrows} \mathbf{1},\mathbf{2}\cdot\mathrm{CB}[5,7] \quad (2)$$

$$\mathbf{1}\cdot\mathrm{CB}[5,7] + \mathrm{CB}[5,7] \overset{K_{1:2}}{\rightleftarrows} \mathbf{1}\cdot(\mathrm{CB}[5,7])_2 \quad (3)$$

where $K_{1:1}$, M^{-1} and $K_{1:2}$, M^{-1} are the stability constants of 1:1 and 1:2 complexes.

In some cases, the accuracy of determination of the stability constants decreases because of too minor spectral changes occurring during the fluorescence titration upon the formation of complex **1**·CB[5]; in the case of spectrophotometric titration and formation of complex **2**@CB[7], accurate determination of the constant is precluded by dimerization, which occurs in parallel. The trends of variation of log$K_{1:1}$ as a function of guest structure and cavitand size thus found are in good agreement with ^{1}H NMR titration data.

3.5. Quantum chemical modeling

Previously, the structure of dye **2** with the Cl$^-$ counterion was calculated by the DFT-D3 method [59]. According to calculations, the free cation is planar and has *Cs* symmetry; this implies the presence of a mirror plane that divides the cation into halves along the *meso*-C–H bond, which results in equalizing the bond orders of the cation. Although the bond lengths and angles are somewhat different in the calculation and the experiment, the principal conclusion about positive charge delocalization in the chromophore is confirmed.

Dye **1** is a trication with three counterions $\mathbf{1}^{3+}\cdot 3ClO_4^-$. In a polar solvent, compound **1** can dissociate stepwise with detachment of perchlorate anions, being converted to positively charged species, $\mathbf{1}^{3+}\cdot 2ClO_4^-$ and $\mathbf{1}^{3+}\cdot ClO_4^-$, respectively. It can be reasonably suggested that $\mathbf{1}^{3+}\cdot 2ClO_4^-$ is present in the solution in the highest concentration. Therefore, in all calculations, we assumed that dye **1** exists in solution as the monocation $\mathbf{1}^{3+}\cdot 2ClO_4^-$, in which each *N*-ammoniohexyl substituent is associated with the perchlorate anion. The structures of complexes were obtained by full geometry optimization by the PM6-DH+ method parameterized to correct structure and energy reproduction for hydrogen-bonded complexes and van der Waals interactions (Figs. 11 and 12).

Comparison of the van der Waals diameter of the CB[5] cavity and the size of the *N*-ammoniohexyl substituent in **1** by the Mercury package interface [60] demonstrated that this residue can penetrate into the cavity. However, the full geometry optimization by the PM6-DH+ method for the complex ($\mathbf{1}^{3+}\cdot 2ClO_4^-$)@CB[5], with one ammoniohexyl substituent in the host–guest starting structure being placed into the CB[5] cavity, resulted in the contact complex in which the ammoniohexyl group is completely displaced from the cavity (Fig. 11*a*) and is hydrogen-bonded to the CB[5] portal. This structure proved to be energetically much more favorable than the chelated structure in which two ammoniohexyl groups embrace the CB[5] portals from two sides (see Fig. 11*b*). Thus, the calculation confirmed the conclusion that follows from analysis of ^{1}H NMR spectra, according to which **1** can form only external contact complex with CB[5].

The insertion of the *N*-ammoniohexyl group into the CB[7] cavity is accompanied by a much higher energy gain giving the expected host–guest type complex. Out of two possible structures, the structure in which the second ammoniohexyl residue is also hydrogen-bonded to the carbonyl CB[7] portal is more favorable (Fig. 11*c*,*d*). These results are consistent with the results of NMR studies (see above).

Quantum chemical calculation also supports the possibility of formation of 1:2 complexes ($\mathbf{1}^{3+}\cdot 2ClO_4^-$)·(CB[5])$_2$ and ($\mathbf{1}^{3+}\cdot 2ClO_4^-$)@(CB[7])$_2$. The insertion of the second *N*-ammoniohexyl substitutent into the cavity of another CB[7] molecule is also accompanied by a large energy gain. The structure of this complex calculated by the PM6-DH+ method is shown in Fig. 12.

It can be seen that the *N*-ammoniohexyl groups of dye **1** are sufficiently flexible, therefore, the formation of complexes with two CB[7] molecules does not produce a sterically strained structure and the chromophore can remain planar, thus retaining the position of the long-wavelength absorption band in the absorption spectrum. In the case of dye **1**, more intense

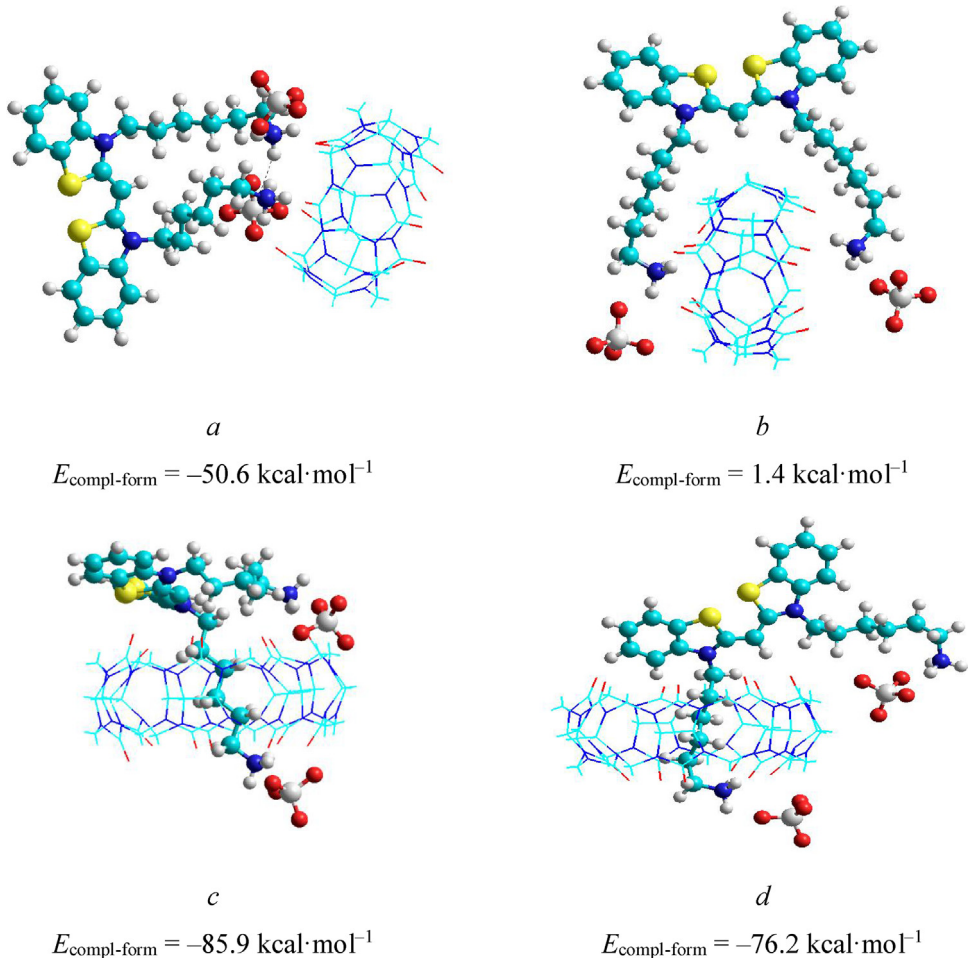

Fig. 11. Structures of complexes ($\mathbf{1}^{3+}$·2ClO_4^-)·CB[5] (*a*,*b*) and ($\mathbf{1}^{3+}$·2ClO_4^-)@CB[7] (*c*,*d*) calculated by the PM6-DH+ method.

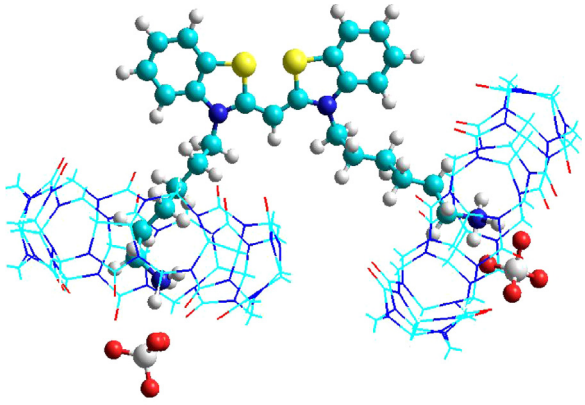

$E_{compl\text{-}form}$ = –98.1 kcal·mol^{-1}.

Fig. 12. Structure of complex ($\mathbf{1}^{3+}$·2ClO_4^-)@(CB[7])$_2$ calculated by the PM6-DH+ method.

fluorescence accompanies the formation of complex **1**@(CB[7])$_2$ (see Table 4). Since the fluorescence band neither shifts nor changes its shape, the increase in the fluorescence intensity is related to a change in the stoichiometry of the CB[7] complex formed. Apparently, in complex **1**@(CB[7])$_2$, the presence of two cavitand molecules results in the rigidity of the environment of the dye chromophore, which hampers the internal conversion of the excited molecule to the ground state.

4. Conclusions

The complexation of monomethine thiacyanine dyes **1** and **2** with CB[5] and CB[7] was studied by spectral methods and by quantum chemical calculations. The stoichiometry, stability, and structure of the supramolecular complexes were determined. The formation of complexes is accompanied by small changes in the absorption spectra and considerable increase in the dye fluorescence intensity, although the chromophore moieties of the dyes are located outside the cavity of the cavitands in all cases. The most pronounced fluorescence enhancement is inherent in the formation of inclusion complexes of the dye with CB[7].

Dye **1** was found to be complexed with CB[5] only *via* binding of the ammonium groups to the carbonyl groups of one of the cavitand portals; however, the *N*-ammoniohexyl groups of dye **1** are able to penetrate inside the CB[7] cavity to form inclusion complexes. The presence of ammonium groups capable of hydrogen bonding in the dye *N*-substituents leads to a considerable increase in the stability of complexes of **1** with CB[5] (by 1.9 orders of magnitude) and CB[7] (by more than 2.5 orders of magnitude) compared with the stability of analogous complexes formed by model dye **2**. Moreover, the presence of two NH_3^+ groups in dye **1** allows for the formation of unusual 1:2 complexes with both cavitands. The results of this study can be useful for targeted design of new types of highly stable photoactive

supramolecular systems involving cyanine dyes and cucurbit[*n*] urils stabilized by the formation of numerous hydrogen bonds, in particular, for the development of optical molecular sensors based on them.

Acknowledgements

Financial support from the Russian Science Foundation (project 14-13-00076 in respect of synthesis of dye **2**), the Russian Foundation for Basic Research (projects 15-03-01883 and 18-03-00214 in respect of self-assembling to supramolecular complexes), and the Russian Academy of Sciences (in respect of X-ray diffraction study of dye **2**) is gratefully acknowledged.

Appendix A. Supplementary data

Supplementary data associated with this article can be found, in the online version, at https://doi.org/10.1016/j.jphotochem.2017.10.035.

References

[1] K. Kim, Mechanically interlocked molecules incorporating cucurbituril and their supramolecular assemblies, Chem. Soc. Rev. 31 (2002) 96–107, doi:http://dx.doi.org/10.1039/A900939F.
[2] O.A. Gerasko, D.G. Samsonenko, V.P. Fedin, Supramolecular chemistry of cucurbiturils, Russ. Chem. Rev. 71 (2002) 741–760, doi:http://dx.doi.org/10.1070/RC2002v071n09ABEH000748.
[3] J.W. Lee, S. Samal, N. Selvapalam, H.-J. Kim, K. Kim, Cucurbituril homologues and derivatives: new opportunities in supramolecular chemistry, Acc. Chem. Res. 36 (2003) 621–630, doi:http://dx.doi.org/10.1021/ar020254k.
[4] W.M. Nau, M. Florea, K.I. Assaf, Deep inside cucurbiturils: physical properties and volumes of their inner cavity determine the hydrophobic driving force for host?guest complexation, Isr. J. Chem. 51 (2011) 559–577, doi:http://dx.doi.org/10.1002/ijch.201100044.
[5] E. Masson, X. Ling, R. Joseph, L. Kyeremeh-Mensah, X. Lu, Cucurbituril chemistry: a tale of supramolecular success, RSC Adv. 2 (2012) 1213–1247, doi:http://dx.doi.org/10.1039/C1RA00768H.
[6] J. Lüa, J.-X. Lin, M.-N. Cao, R. Cao, Cucurbituril: a promising organic building block for the design of coordination compounds and beyond, Coord. Chem. Rev. 257 (2013) 1334–1356, doi:http://dx.doi.org/10.1016/j.ccr.2012.12.014.
[7] S. Zarra, D.M. Wood, D.A. Roberts, J.R. Nitschke, Molecular containers in complex chemical systems, Chem. Soc. Rev. 44 (2015) 419–432, doi:http://dx.doi.org/10.1039/C4CS00165F.
[8] K.I. Assaf, W.M. Nau, Cucurbiturils: from synthesis to high-affinity binding and catalysis, Chem. Soc. Rev. 44 (2015) 394–418, doi:http://dx.doi.org/10.1039/C4CS00273C.
[9] E. Arunkumar, C.C. Forbes, B.D. Smith, Improving the properties of organic dyes by molecular encapsulation, Eur. J. Org. Chem. (2005) 4051–4059, doi:http://dx.doi.org/10.1002/ejoc.200500372.
[10] A.L. Koner, W.M. Nau, Cucurbituril encapsulation of fluorescent dyes, Supramol. Chem. 19 (2007) 55–66, doi:http://dx.doi.org/10.1080/10610270600910749.
[11] R.N. Dsouza, U. Pischel, W.M. Nau, Fluorescent dyes and their supramolecular host/guest complexes with macrocycles in aqueous solution, Chem. Rev. 111 (2011) 7941–7980, doi:http://dx.doi.org/10.1021/cr200213s.
[12] S. Gadde, E.K. Batchelor, J.P. Weiss, Y. Ling, A.E. Kaifer, Control of H- and J-aggregate formation via host–guest complexation using cucurbituril hosts, J. Am. Chem. Soc. 130 (2008) 17114–17119, doi:http://dx.doi.org/10.1021/ja807197c.
[13] S. Gadde, E.K. Batchelor, A.E. Kaifer, Controlling the formation of cyanine dye H- and J-aggregates with cucurbituril hosts in the presence of anionic polyelectrolytes, Chem. –Eur. J. 15 (2009) 6025–6031, doi:http://dx.doi.org/10.1002/chem.200802546.
[14] H. Zhang, L. Liu, C. Gao, R. Sun, Q. Wang, Enhancing photostability of cyanine dye by cucurbituril encapsulation, Dyes Pigm. 94 (2012) 266–270, doi:http://dx.doi.org/10.1016/j.dyepig.2012.01.022.
[15] N. Barooah, J. Mohanty, H. Pal, A.C. Bhasikuttan, Stimulus-responsive supramolecular pKa tuning of cucurbit[7] uril encapsulated coumarin 6 dye, J. Phys. Chem. B 116 (2012) 3683–3689, doi:http://dx.doi.org/10.1021/jp212459r.
[16] W.M. Nau, J. Mohanty, Taming fluorescent dyes with cucurbituril, Int. J. Photoenergy 7 (2005) 133–141, doi:http://dx.doi.org/10.1155/S1110662X05000206.
[17] G. Parvari, O. Reany, E. Keinan, Applicable properties of cucurbiturils, Isr. J. Chem. 51 (2011) 646–663, doi:http://dx.doi.org/10.1002/ijch.201100048.
[18] A.C. Bhasikuttan, H. Pal, J. Mohanty, Cucurbit[n]uril based supramolecular assemblies: tunable physico-chemical properties and their prospects, Chem. Commun. 47 (2011) 9959–9971, doi:http://dx.doi.org/10.1039/C1CC12091C.
[19] A.C. Bhasikuttan, S.D. Choudhury, H. Pal, J. Mohanty, Supramolecular assemblies of thioflavin T with cucurbiturils: prospects of cooperative and competitive metal ion binding, Isr. J. Chem. 51 (2011) 634–645, doi:http://dx.doi.org/10.1002/ijch.201100039.
[20] Z. Li, S. Sun, F. Liu, Y. Pang, J. Fan, F. Song, X. Penga, Large fluorescence enhancement of a hemicyanine by supramolecular interaction with cucurbit[6] uril and its application as resettable logic gates, Dyes Pigm. 93 (2012) 1401–1407, doi:http://dx.doi.org/10.1016/j.dyepig.2011.10.005.
[21] J. Mohanty, N. Thakur, S.D. Choudhury, N. Barooah, H. Pal, A.C. Bhasikuttan, Recognition-mediated light-up of thiazole orange with cucurbit[8] uril: exchange and release by chemical stimuli, J. Phys. Chem. B 116 (2012) 130–135, doi:http://dx.doi.org/10.1021/jp210432t.
[22] S.J. Barrow, S. Kasera, M.J. Rowland, J. del Barrio, O.A. Scherman, Cucurbituril-based molecular recognition, Chem. Rev. 115 (2015) 12320–12406, doi:http://dx.doi.org/10.1021/acs.chemrev.5b00341.
[23] L.G. Kuz'mina, A.I. Vedernikov, N.A. Lobova, J.A.K. Howard, Yu.A. Strelenko, V.P. Fedin, M.V. Alfimov, S.P. Gromov, Photoinduced and dark complexation of unsaturated viologen analogues containing two ammonium tails with cucurbit[8] uril, New J. Chem. 30 (2006) 458–466, doi:http://dx.doi.org/10.1039/B511456J.
[24] A.I. Vedernikov, N.A. Lobova, L.G. Kuz'mina, J.A.K. Howard, Yu.A. Strelenko, M. V. Alfimov, S.P. Gromov, Pseudorotaxane complexes between viologen vinylogues and cucurbit[7] uril: new prototype of photocontrolled molecular machine, J. Mol. Struct. 989 (2011) 114–121, doi:http://dx.doi.org/10.1016/j.molstruc.2011.01.013.
[25] N.Kh. Petrov, D.A. Ivanov, D.V. Golubkov, S.P. Gromov, M.V. Alfimov, The effect of cucurbit[7]uril on photophysical properties of aqueous solution of 3,3-diethylthiacarbocyanine iodide dye, Chem. Phys. Lett. 480 (2009) 96–99, doi:http://dx.doi.org/10.1016/j.cplett.2009.08.042.
[26] G.V. Zakharova, D.A. Zhizhimov, S.K. Sazonov, V.G. Avakyan, S.P. Gromov, H. Görner, A.K. Chibisov, Photoprocesses of alkyl meso-thiacarbocyanine dyes in the presence of cucurbit[7] uril, J. Photochem. Photobiol. A: Chem. 302 (2015) 69–77, doi:http://dx.doi.org/10.1016/j.jphotochem.2015.01.011.
[27] S.P. Gromov, A.I. Vedernikov, L.G. Kuz'mina, D.V. Kondratuk, S.K. Sazonov, Yu.A. Strelenko, M.V. Alfimov, J.A.K. Howard, Photocontrolled molecular assembler based on cucurbit[8] uril: [2 + 2]-autophotocycloaddition of styryl dyes in the solid state and in water, Eur. J. Org. Chem. (2010) 2587–2599, doi:http://dx.doi.org/10.1002/ejoc.200901324.
[28] D.A. Ivanov, N.Kh. Petrov, E.A. Nikitina, M.V. Basilevsky, A.I. Vedernikov, S.P. Gromov, M.V. Alfimov, The 1:1 host–guest complexation between cucurbit[7] uril and styryl dye, J. Phys. Chem. A 115 (2011) 4505–4510, doi:http://dx.doi.org/10.1021/jp1123579.
[29] L.S. Atabekyan, A.I. Vedernikov, V.G. Avakyan, N.A. Lobova, S.P. Gromov, A.K. Chibisov, Photoprocesses in styryl dyes and their pseudorotaxane complexes with cucurbit[7] uril, J. Photochem. Photobiol. A: Chem. 253 (2013) 52–61, doi:http://dx.doi.org/10.1016/j.jphotochem.2012.12.023.
[30] D.A. Ivanov, N.Kh. Petrov, M.V. Alfimov, A.I. Vedernikov, S.P. Gromov, Supramolecular assembler based on cucurbit[8]uril: photodimerization of a styryl dye in water, High Energy Chem. 48 (2014) 253–259, doi:http://dx.doi.org/10.1134/S0018143914040079.
[31] D.A. Ivanov, N.Kh. Petrov, A.A. Ivanov, M.V. Alfimov, A.I. Vedernikov, S.P. Gromov, A fast relaxation of electronically-excited inclusion complexes of a styryl dye with cucurbit[7] uril, Chem. Phys. Lett. 610–611 (2014) 91–94, doi:http://dx.doi.org/10.1016/j.cplett.2014.07.006.
[32] A.I. Vedernikov, N.A. Lobova, N.A. Aleksandrova, S.P. Gromov, Study of complexation of styrylheterocycles with cavitands by spectroscopic methods, Russ. Chem. Bull. 64 (2015) 2459–2472, doi:http://dx.doi.org/10.1007/s11172-015-1178-x.
[33] A.D. Svirida, D.A. Ivanov, N.Kh. Petrov, A.V. Vedernikov, S.P. Gromov, M.V. Alfimov, Photophysical properties of aqueous solutions of a styryl dye in the presence of cucurbit[n]uril (n = 5, 6, 8), High Energy Chem. 50 (2016) 21–26, doi:http://dx.doi.org/10.1134/S0018143916010094.
[34] N.Kh. Petrov, D.A. Ivanov, Yu.A. Shandarov, I.V. Kryukov, A.A. Ivanov, M.V. Alfimov, N.A. Lobova, S.P. Gromov, Ultrafast relaxation of electronically-excited states of a styryl dye in the cavity of cucurbit[n]urils (n = 6, 7), Chem. Phys. Lett. 647 (2016) 157–160, doi:http://dx.doi.org/10.1016/j.cplett.2016.01.063.
[35] L. Isaacs, S.-K. Park, S.M. Liu, Y.H. Ko, N. Selvapalam, Y. Kim, H. Kim, P.Y. Zavalij, G.-H. Kim, H.-S. Lee, K. Kim, The inverted cucurbit[n]uril family, J. Am. Chem. Soc. 127 (2005) 18000–18001, doi:http://dx.doi.org/10.1021/ja056988k.
[36] J. Kim, I.-S. Jung, S.-Y. Kim, E. Lee, J.-K. Kang, S. Sakamoto, K. Yamaguchi, K. Kim, New cucurbituril homologues: syntheses, isolation, characterization, and X-ray crystal structures of cucurbit[n]uril (n = 5, 7, and 8), J. Am. Chem. Soc 122 (2000) 540–541, doi:http://dx.doi.org/10.1021/ja993376p.
[37] S. Liu, X. Wu, Z. Huang, J. Yao, F. Liang, C. Wu, Construction of pseudorotaxanes and rotaxanes based on cucurbit[n]uril, J. Incl. Phenom. Macrocycl. Chem. 50 (2004) 203–207, doi:http://dx.doi.org/10.1007/s10847-004-6472-4.
[38] J. Lagona, P. Mukhopadhyay, S. Chakrabarti, L. Isaacs, The cucurbit[n]uril family, Angew. Chem. Int. Ed. 44 (2005) 4844–4870, doi:http://dx.doi.org/10.1002/anie.200460675.
[39] Y. Kim, H. Kim, Y.H. Ko, N. Selvapalam, M.V. Rekharsky, Y. Inoue, K. Kim, Complexation of aliphatic ammonium ions with a water-soluble cucurbit[6] uril derivative in pure water: isothermal calorimetric, NMR, and X-ray crystallographic study, Chem. –Eur. J. 15 (2009) 6143–6151, doi:http://dx.doi.org/10.1002/chem.200900305.
[40] K. Jansen, H.-J. Buschmann, A. Wego, D. Döpp, C. Mayer, H.-J. Drexler, H.-J. Holdt, E. Schollmeyer, Cucurbit[5] uril, decamethylcucurbit[5] uril and

cucurbit[6] uril Synthesis, solubility and amine complex formation, J. Incl. Phenom. Macrocycl. Chem. 39 (2001) 357–363, doi:http://dx.doi.org/10.1023/A:1011184725796.
[41] S.P. Gromov, M.V. Fomina, A.S. Nikiforov, A.I. Vedernikov, L.G. Kuz'mina, J.A.K. Howard, Synthesis of symmetrical cyanine dyes with two N-ammonioalkyl groups, Tetrahedron 69 (2013) 5898–5907, doi:http://dx.doi.org/10.1016/j.tet.2013.05.015.
[42] M.V. Fomina, A.S. Nikiforov, S.P. Gromov, Modern approaches to the synthesis and prospects for the use of cyanine dyes containing functional groups in the N-substituents, Russ. Chem. Rev. 85 (2016) 684–699, doi:http://dx.doi.org/10.1070/RCR4585.
[43] D.M. Fabricius, R.J. Le Strange, Blue spectral sensitizers for non-tabular silver halide elements, EP 467155 A1, 1992, Chem. Abstr. 116 (1992) 265435.
[44] A.I. Vedernikov, E.N. Ushakov, N.A. Lobova, A.A. Kiselev, M.V. Alfimov, S.P. Gromov, Photosensitive molecular tweezers. 3. Synthesis and homoditopic complex formation of a bisstyryl dye containing two crown-ether fragments with diammonium salts, Russ. Chem. Bull. 54 (2005) 666–672, doi:http://dx.doi.org/10.1007/s11172-005-0303-7.
[45] G.M. Sheldrick, Crystal structure refinement with SHELXL, Acta Crystallogr. Sect. C 71 (2015) 3–8, doi:http://dx.doi.org/10.1107/S2053229614024218.
[46] C. Frassineti, S. Ghelli, P. Gans, A. Sabatini, M.S. Moruzzi, A. Vacca, Nuclear magnetic resonance as a tool for determining protonation constants of natural polyprotic bases in solution, Anal. Biochem. 231 (1995) 374–382, doi:http://dx.doi.org/10.1006/abio.1995.9984.
[47] P. Gans, A. Sabatini, A. Vacca, Investigation of equilibria in solution. Determination of equilibrium constants with the HYPERQUAD suite of programs, Talanta 43 (1996) 1739–1753, doi:http://dx.doi.org/10.1016/0039-9140(96)01958-3.
[48] J.D.C. Maia, G.A.U. Carvalho, C.P. Mangueira Jr., S.R. Santana, L.A.F. Cabral, G.B. Rocha, GPU. Linear algebra libraries and GPGPU programming for accelerating MOPAC semiempirical quantum chemistry calculations, J. Chem. Theory Comput. 8 (2012) 3072–3081, doi:http://dx.doi.org/10.1021/ct3004645.
[49] MOPAC2012, J.J.P. Stewart, Stewart Computational Chemistry, Version 15.038W, Colorado Springs, CO, USA, 2012. http://OpenMOPAC.net.
[50] J. Dalwing, D. Hagen, T. Huang, J. Thomas, S. Yue, WO patent 2005056689, 2005, Chem. Abstr. 143 (2005) 61414.
[51] H. Stoeckli-Evans, The crystal structure of 5,5′,7,7′-tetramethyl-3,3′,9-triethyl thiacarbocyanine perchlorate, Helv. Chim. Acta 57 (1974) 1–9, doi:http://dx.doi.org/10.1002/hlca.19740570102.
[52] K. Nakao, K. Yakeno, H. Yoshioka, K. Nakatsu, Crystal structure of a methanol solvate of 3, 3(-diethyl-9-phenylthiacarbocyanine iodide, a photographic sensitizing dye, Acta Crystallogr. Sect. B 35 (1979) 415–419, doi:http://dx.doi.org/10.1107/S05677408790036.
[53] M.C. Grossel, F.A. Evans, J.A. Hriljac, K. Prout, S.C. Weston, Triplet excitons in isolated TCNQ–dimers (TCNQ = tetracyanoquinodimethane), J. Chem. Soc. Chem. Commun. (1990) 1494–1495, doi:http://dx.doi.org/10.1039/C39900001494.
[54] L.M. Yagupolskii, N.V. Kondratenko, O.I. Chernega, A.N. Chernega, S.A. Buth, Yu. L. Yagupolskii, A novel synthetic route to thiacyanine dyes containing a perfluorinated polymethine chain, Dyes Pigm. 79 (2008) 242–246, doi:http://dx.doi.org/10.1016/j.dyepig.2008.03.003.
[55] T.H. James, The Theory of the Photographic Process, 4th ed., MacMillan Co., New York, 1977, pp. 1–715.
[56] V.I. Yuzhakov, Aggregation of dye molecules and its influence on the spectral luminescent properties of solutions, Russ. Chem. Rev. 61 (1992) 613–628, doi:http://dx.doi.org/10.1070/RC1992v061n06ABEH000988.
[57] A.K. Chibisov, G.V. Zakharova, H. Görner, Photoprocesses of thiamonomethinecyanine monomers and dimers, Phys. Chem. Chem. Phys. 3 (2001) 44–49, doi:http://dx.doi.org/10.1039/B005683I.
[58] A.K. Chibisov, Photonics of dimers of cyanine dyes, High Energy Chem. 41 (2007) 200–209, doi:http://dx.doi.org/10.1134/S0018143907030071.
[59] V.G. Avakyan, B.I. Shapiro, M.V. Alfimov, Dimers, tetramers, and octamers of mono- and trimethine thiacarbocyanine dyes. Structure, formation energy, and absorption band shifts, Dyes Pigm. 109 (2014) 21–33, doi:http://dx.doi.org/10.1016/j.dyepig.2014.04.026.
[60] Mercury 3.9 (Build RC1) http://www.ccdc.cam.ac.uk/mercury/